Effect of Adsorbed Polyelectrolytes on Nanoscale Zero Valent Iron Particle Attachment to Soil Surface Models

KEVIN M. SIRK,[†] NAVID B. SALEH,[‡] TANAPON PHENRAT,[‡] HYE-JIN KIM,[‡] BRUNO DUFOUR,[§] JEONGBIN OK,[§] PATRICIA L. GOLAS,[§] KRZYSZTOF MATYJASZEWSKI,[§] GREGORY V. LOWRY,[‡] AND ROBERT D. TILTON*[,†,∥]

Center for Environmental Implications of Nanotechnology and Departments of Chemical Engineering, Civil and Environmental Engineering, Chemistry, and Biomedical Engineering, Carnegie Mellon University, Pittsburgh, Pennsylvania 15213

Received December 18, 2008. Revised manuscript received February 18, 2009. Accepted March 20, 2009.

Polyelectrolyte coatings significantly increase the mobility of nanoscale zerovalent iron (NZVI) in saturated porous media. The effect can be attributed to improved colloidal stability of NZVI suspensions, decreased adhesion to soil surfaces, or a combination of the two effects. This research explicitly examines how coatings control NZVI adhesion to model soil surfaces. NZVI was coated with three different polyelectrolyte block copolymers based on poly(methacrylic acid), poly(methyl methacrylate or butyl methacrylate), and poly(styrenesulfonate) or with a poly(styrenesulfonate) homopolymer. SiO_2 and a humic acid film served as model soil surfaces. The polyelectrolytes increased the magnitude of the electrophoretic mobility of NZVI over a broad pH range relative to unmodified NZVI and shifted the isoelectric point outside the typical groundwater pH range. Quartz crystal microgravimetry measurements indicated extensive adhesion of unmodified NZVI to SiO_2. Polyelectrolyte coatings decreased adhesion by approximately 3 orders of magnitude. Adding 50 mM NaCl to screen electrostatic repulsions did not significantly increase adhesion of modified NZVI. Coated NZVI did not adhere to humic acid films for either 1 mM $NaHCO_3$ or 1 mM $NaHCO_3$ + 50 mM NaCl. The lack of adhesion even in a high ionic strength medium was attributed to electrosteric repulsion, as opposed to electrostatic double layer repulsion, between the polyelectrolyte-coated NZVI and the negatively charged surfaces. The lack of significant adhesion on either model surface was observed for all polymer architectures investigated.

Introduction

$Fe^{(0)}$ nanoparticles, or NZVI, are proposed as a groundwater remediation technology to immobilize toxic metals (*1*) and to dechlorinate dense, nonaqueous phase liquid (DNAPL) contaminants. NZVI oxidation in the presence of water reduces DNAPL contaminants to less toxic or immobile products (*2*−*5*). NZVI offers high reactivity mainly due to large specific surface areas (*2*). Because of the small particle size relative to subsurface pores, NZVI also offers the potential to be transported in groundwater, perhaps even to be targeted and emplaced in subsurface source zones. Yet, recent research has shown that unmodified NZVI suspensions transport poorly through water-saturated sand columns (*6*−*11*).

Several strategies have been proposed to promote NZVI transport, such as emulsifying NZVI in vegetable oil (*12*), or attaching NZVI to 50−200 nm hydrophilic, anionic carbon supports (*8*). Another approach is to directly modify the surfaces of individual NZVI particles to enhance their stability and transport (*13*). Adsorbed poly(acrylic acid) (*8*) and carboxymethylcellulose (*7*) have been shown to significantly enhance NZVI elution from sand columns.

We have used a novel triblock copolymer architecture as a surface modifier, poly(methacrylic acid)-*block*-(methyl methacrylate or butyl methacrylate)-*block*-(styrenesulfonate) (PMAA-PMMA-PSS or PMAA-PBMA-PSS), that can enhance NZVI dispersion stability (*14, 15*), increase mobility in porous media (*9*), and promote pollutant targetability (*9, 14*). The triblock copolymers were designed to incorporate multiple functions within a single polymer chain. Since carboxylic acids bind strongly to iron oxide surfaces (*16, 17*), the PMAA block is intended to strongly anchor the copolymer to the NZVI surface. The PMMA (or PBMA) block is hydrophobic and renders the polymer coating amphiphilic, so that it might anchor the particle to the water/DNAPL interface (*9, 14*). The PSS block has two functions. Highly water-soluble, it serves as a NZVI dispersant. Second, since most soil minerals, whether bare or coated by natural organic matter (NOM), are negatively charged, the anionic PSS block provides electrosteric repulsion between NZVI and groundwater solids. PSS is a strong polyelectrolyte, with ionization independent of pH. Adsorbed layers of such "quenched" polyelectrolytes provide electrosteric repulsions that are strong and robust, persisting to high ionic strengths where simple electrostatic double layer repulsions fail (*18*−*20*). The repulsion arises from increased osmotic pressure associated with polymer chain confinement and ion redistributions when the layer is compressed. We previously showed that adsorbed PMAA−PMMA−PSS triblock copolymers enabled >95% NZVI elution from saturated sand columns, compared to ∼1% for unmodified NZVI (*9*).

To transport effectively in groundwater, NZVI must resist aggregation and straining, as well as hydrodynamic and/or gravitational deposition into adhesive contact with solid surfaces (*13*). Here, we used the quartz crystal microgravimetry with dissipation (QCM-D) technique (*21, 22*) to monitor the direct adhesion of NZVI to bare silica surfaces and to humic acid films in order to simulate the surfaces of groundwater media for environmentally relevant solution ionic conditions (1−50 mM Na^+). Since block copolymer architecture is well-known to control the conformation of adsorbed polymer layers and the resulting colloidal forces, we employed the family of PMAA−PMMA−PSS block copolymers described by Saleh and co-workers (*9, 14*) with systematically varied block content to develop design rules for the most effective elimination of adhesion to model groundwater solids. Surprisingly, all of the PSS-containing polymers prevent NZVI adhesion to both silica and humic acid films with equal effectiveness. This is attributed to the

* Corresponding author phone: 412-268-1159; e-mail: tilton@andrew.cmu.edu.
[†] Department of Chemical Engineering.
[‡] Department of Civil and Environmental Engineering.
[§] Department of Chemistry.
[∥] Department of Biomedical Engineering.

10.1021/es803589t CCC: $40.75
Published on Web 04/08/2009

strong electrosteric repulsions imparted by PSS. Evidently, these repulsions are sufficiently strong to eliminate adhesion regardless of how the polymer architecture determines the conformation of the adsorbed layers. As a result, one may have considerable freedom in designing polymers for source-zone delivery, provided that it contains a strong anionic polyelectrolyte block.

Experimental Section

Materials. All samples were prepared using reverse osmosis water that was further purified to 18 MΩ·cm resistivity by an Easypure II system (Barnstead). $NaHCO_3$ (Sigma), NaCl (Fisher Chemicals), octadecyltrichlorosilane (OTS, Aldrich), concentrated HCl (trace metal grade, Fisher Chemicals), concentrated HNO_3 (trace metal grade, Fisher Chemicals), humic acid from coal tar (ACROS), and poly(sodium-4-styrenesulfonate) with $M_w = 70\,000$ g/mol (Aldrich) were all used as received. Reactive nano-iron particles (RNIP) provided by Toda Kogyo (Onada, Japan) were used as the NZVI. RNIP has a $Fe^{(0)}$ core with a predominantly Fe_3O_4 shell (*2*). The specific surface area for these particles, measured using the BET method (Quantachrome, NOVAe), was 4.9 ± 0.4 m^2/g. This is lower than the manufacturer reports, most likely because of the RNIP aging process described below. Further RNIP characterization information is published elsewhere (*2, 6*).

Atom transfer radical polymerization (*23, 24*) was used to synthesize three different block copolymers: poly(methacrylic acid)-poly(styrenesulfonate) and poly(methyl methacrylate)-poly(styrenesulfonate) diblocks, and a poly(methacrylic acid)-poly(butyl methacrylate)-poly(styrenesulfonate) triblock copolymer. Synthesis methods are described in the Supporting Information.

Materials and Methods. *Sample Preparation.* Adsorption isotherms for each polymer on RNIP were measured by the solution depletion method using suspensions in polypropylene centrifuge tubes. RNIP suspensions were made by diluting a 10 mL aliquot taken from the 300 g/L stock slurry to 400 mL in deionized H_2O. This diluted stock suspension was stored for several weeks until visible H_2 production from oxidation of the available $Fe^{(0)}$ ceased. This was done to ensure that the RNIP surface chemistry and solution pH would not change during the time allowed for polymer adsorption. This diluted stock RNIP suspension was then dispersed by ultrasonication for 20 min using a sonic dismembrator (model 550, Fisher Scientific). For each polymer used, 8 mL samples were prepared in the centrifuge tube to contain polymer concentrations ranging from 0.02 to 1.2 mg/mL. With the diluted RNIP suspension under constant sonication, 4 mL aliquots were placed into each tube, bringing the final volume to 12 mL. The final electrolyte content was either 1 mM $NaHCO_3$ or 1 mM $NaHCO_3$ + 50 mM NaCl. The NaCl was added to some samples to screen electrostatic double layer repulsions to investigate the role they play in polyelectrolyte adsorption and RNIP adhesion.

RNIP was always added last in the sample preparation sequence. Each sample was then ultrasonicated for 1 min, capped and rotated end-over-end at 20 rpm for 48 h to allow the polymer to adsorb. Experiments with shorter rotation times confirmed that 48 h was sufficient to saturate the polymer adsorption to RNIP. Not independently controlled, the natural pH of the RNIP/polymer mixtures ranged from 6.5 to 7.5, always above the RNIP isoelectric point (see below).

Iron Analysis. After 48 h of rotation, 2 mL aliquots were taken from each sample to determine the iron content via flame atomic absorption (GBC 908AA). Each aliquot was mixed with 6 mL of concentrated HCl in a glass scintillation vial. After acid digestion, 6 mL of deionized water was added to each solution, which had turned yellow. From these samples, triplicate 0.2 mL aliquots were taken and diluted with 10 mL of 1% HNO_3. These samples were then analyzed via flame atomic absorption and then the total mass of particles (as iron) added to each sample was determined. The total RNIP particle mass was determined by multiplying the total iron by a factor of 1.31 that accounts for the ~9% $Fe^{(0)}$ content of this aged RNIP, with the remainder iron oxide (*3*).

Polymer Adsorption Isotherms. After the iron measurement, the remaining 10 mL of each polymer/RNIP mixture was then centrifuged (Sorvall Ultracentrifuge OTD65B) for 1.5 h at 27 500 rpm to completely settle the RNIP. After centrifugation, supernatant aliquots were taken and diluted to measure the free polymer concentration in solution by its absorbance at 225 nm (Varian Cary 300), based on a separately determined calibration curve for each polymer. Lack of spectrophotometric interference from dissolved iron was verified by comparing the full supernatant spectrum to that of pure polyelectrolyte solutions in iron-free water. Subtracting the free polymer concentration from the original bulk concentration yielded the adsorbed amount. Surface concentrations were calculated from the measured RNIP concentration and 4.9 ± 0.4 m^2/g specific surface area. All RNIP samples to be used for electrophoretic mobility or QCM-D experiments were centrifuged and washed four times to ensure complete removal of nonadsorbed polymers from solution, leaving only polymer irreversibly adsorbed on RNIP. Polymer adsorption is typically irreversible. Had polymer desorption been significant, it would have been evident by a resulting aggregation of the NZVI suspensions (*6*). This did not occur.

Electrophoretic Mobility vs pH. Several 25 mg/L suspensions of bare or polymer modified RNIP in 1 mM $NaHCO_3$ were made and small aliquots of either HCl or NaOH were added to adjust the pH to between ~3.5 and 10. Five replicate electrophoretic mobility measurements were made with a Malvern Zetasizer 3000.

QCM-D. To monitor RNIP adhesion to silica or humic acid films, we used the QCM-D instrument from QSense (D300, Göteborg, Sweden), which is described in detail elsewhere (*18*). In a QCM-D experiment, there are four separate resonance frequencies (overtones, *n*) for the driven oscillation of the shear wave through an AT cut quartz crystal, with the gold electrode coated with an overlayer of SiO_2: 5 MHz ($n = 1$), 15 MHz ($n = 3$), 25 MHz ($n = 5$), and 35 MHz ($n = 7$). As mass is adsorbed from the bulk fluid to the crystal surface, each of the resonance frequencies decreases. If the adsorbed layer is uniformly distributed, rigidly attached, and small compared to the mass of the crystal, the change in frequency (Δf) can be related to the sensed adsorbed mass per unit area (Δm) using the Sauerbrey relation (*25*):

$$\Delta m = -\frac{C\Delta f}{n} \tag{1}$$

where C is an instrument constant related to the properties of the crystal (in our case $C = 0.177$ mg m^{-2} Hz^{1-}). In all of the experiments, the data from the third overtone was used to calculate the adsorbed mass. The QCM-D "sensed" mass represents the mass of adherent particles plus the bound water in the adsorbed layer (*22*).

Silica-coated crystals were purchased from Q-Sense and cleaned immediately before use as follows: crystals were placed in a UV-Ozone chamber (Jelight Co., Irving, CA) for 90 min and then immersed in Chromerge (Fisher Scientific) CrO_3/H_2SO_4 cleaning solution for 30 min followed by copious rinsing with deionized water. Crystals were blown dry with N_2. All experiments were performed at 25 ± 0.1 °C.

Before injecting samples, a stable baseline was recorded for at least 2 min with the appropriate background solution (1 mM $NaHCO_3$ or 1 mM $NaHCO_3$ + 50 mM NaCl) in the cell. Then, 2 mL of RNIP suspension were injected through the

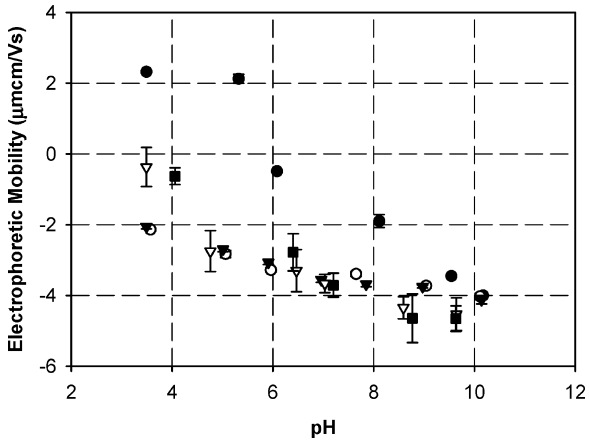

FIGURE 1. pH dependence of electrophoretic mobility for 25 mg/L suspensions of (●) bare RNIP, and RNIP modified with irreversibly adsorbed (■) PSS_{339}, (▽) $PMMA_{45}$-PSS_{609}, (○) $PMAA_{15}$-PSS_{811}, and (▼) $PMAA_{15}$-$PBMA_{43}$-PSS_{811} in 1 mM $NaHCO_3$.

cell (corresponding to 25 cell volumes) to ensure complete displacement of the background solution. Any subsequent adhesion was monitored for at least one hour. The RNIP concentration was 0.2 wt% in all adhesion measurements. This concentration is in the typical range appropriate for groundwater remediation (*6, 13*).

For the humic acid studies, cleaned crystals were immersed in a 3 mM solution of OTS in a 90:10 hexadecane: chloroform mixture for 45 min to produce an uncharged, hydrophobic alkane monolayer (*26*). Crystals were then rinsed with excess chloroform and blown dry with N_2. This hydrophobization step was necessary to deposit a stable humic acid film on the crystals. Humic acid solutions of initial concentration 0.4 mg/mL were filtered with a 0.45 μm filter prior to use. After mounting the hydrophobized crystal in the QCM-D, a 1 mM $NaHCO_3$ solution was injected to collect the baseline, after which 2 mL of the humic acid solution was injected and allowed to adsorb for at least one hour. Then fresh $NaHCO_3$ solution was injected to remove any free humic acid from the system. This deposition and rinse procedure was repeated twice before injecting RNIP suspensions.

Results and Discussion

Electrophoretic Mobility and Adsorption Isotherms of Polymer Modified RNIP. Figure 1 presents the electrophoretic mobility of bare RNIP, $PMAA_{15}$-$PBMA_{43}$-PSS_{811}, $PMAA_{15}$-PSS_{811}, $PMMA_{45}$-PSS_{609}, and PSS_{339} modified RNIP as a function of pH (subscripts denote the degree of polymerization for each block). The isoelectric point for the bare particles was slightly below pH 6. Adsorption of any of the polyelectrolytes increased the negative electrophoretic mobility and shifted the isoelectric point to below pH 3 (beyond the pH range investigated). Thus, any of the polyelectrolyte modifiers should enhance the electrostatic repulsion between RNIP and other similarly charged surfaces, for any pH likely to be found in typical groundwater.

Adsorption isotherms are plotted in Figure 2 for $PMAA_{15}$-$PBMA_{43}$-PSS_{811} and $PMAA_{15}$-PSS_{811} on RNIP in 1 mM $NaHCO_3$. The maximum attained surface excess concentrations for $PMAA_{15}$-$PBMA_{43}$-PSS_{811} triblocks and $PMAA_{15}$-PSS_{811} diblocks are 1.6 ± 0.3 mg/m^2 and 0.34 ± 0.1 mg/m^2, respectively. The presence of the hydrophobic PBMA block, with otherwise identical PMAA (anchor) and PSS (stabilizing) blocks, promotes a 5-fold increase in adsorbed mass. Hydrophobic attractions among the adsorbed PBMA blocks evidently create a higher areal density of chains on the surface that would lead to greater PSS chain extension. This effect would promote stronger, longer ranged electrosteric repulsions (*15*).

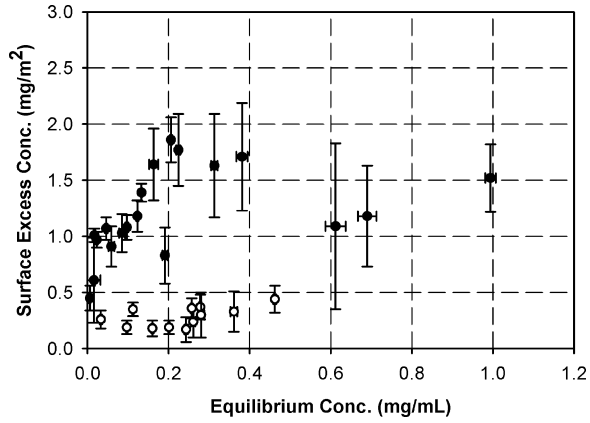

FIGURE 2. Adsorption isotherms of $PMAA_{15}$-PSS_{811} (○ open circles) and $PMAA_{15}$-$PBMA_{43}$-PSS_{811} (●closed circles). The samples were in 1 mM $NaHCO_3$ solution.

Adsorption isotherms for the same two polymers adsorbed at a higher ionic strength, 1 mM $NaHCO_3$ + 50 mM NaCl, yielded maximum surface excess concentrations of 2.8 ± 0.6 mg/m^2 and 0.7 ± 0.2 mg/m^2 for the triblock and diblock respectively (data in the Supporting Information). Increasing ionic strength more effectively screens interchain electrostatic repulsions and allows the polymers to pack closer together.

We also adsorbed PSS_{339} homopolymer and $PMMA_{45}$-PSS_{609} diblock copolymer to RNIP in 1 mM $NaHCO_3$ and found the maximum surface excess concentrations to be 0.26 ± 0.03 mg/m^2 and 1.3 ± 0.4 mg/m^2 respectively (Data in the Supporting Information). Noting that the adsorbed amount of polyelectrolyte homopolymers is typically independent of molecular weight (*27, 28*), the similar adsorbed amounts attained for $PMAA_{15}$-PSS_{811} (0.34 ± 0.1 mg/m^2) and PSS_{339} (0.26 ± 0.03 mg/m^2) indicate that the PMAA block had little influence on the adsorption. In the case of the amphiphilic $PMMA_{45}$-PSS_{609} diblock copolymer, the hydrophobic PMMA block was able to displace adsorbed PSS segments from the surface, forcing them to adopt a more extended conformation stretching away from the surface, and thereby allowing the greater adsorbed amount for the diblock relative to the homopolymer. In the case of the hydrophilic $PMAA_{15}$-PSS_{811} diblock copolymer, the affinity of the PMAA block for the iron oxide surface was not sufficient to displace PSS segments, and the entire chain lay relatively flat on the surface, resulting in an indistinguishable amount of adsorption relative to the PSS homopolymer that would also lay in a relatively flat conformation.

Although these results show that the PMAA block had little effect on the adsorbed amount, such a block does appear to help promote triblock copolymer-modified RNIP attachment to the water/TCE interface as noted by Saleh et al. (*14*). Previously, Sontum and co-workers (*29*) measured PSS homopolymer adsorption on positively charged iron oxide particles at pH 4 and estimated the surface excess concentration to be 26 mg/m^2. They attributed the unusually high adsorbed amount to multilayer adsorption. On the negatively charged RNIP surfaces, the measured adsorbed amounts we obtained indicate monolayer adsorption for PSS. In summary, the adsorption isotherm measurements indicate that amphiphilic diblock and triblock copolymers containing PSS adopt a more extended conformation on the surface, while hydrophilic PMAA-PSS diblock and PSS homopolymers adopt a flatter conformation on the surface. Differences in adsorbed polyelectrolyte surface excess concentration and conformation are known to control the strength and range of electrosteric repulsion forces (*18–20*), leading one to anticipate differences in the adhesion resistance of RNIP modified by these different polyelectrolytes.

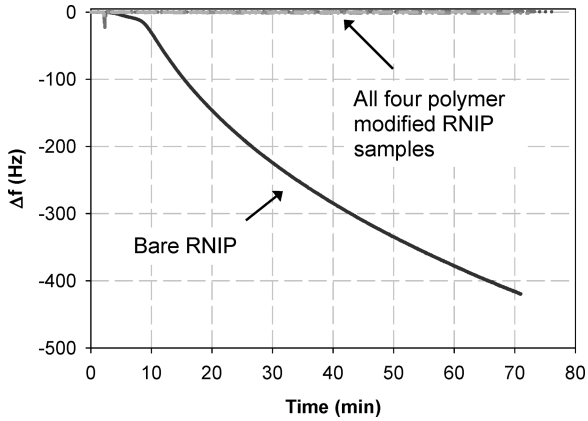

FIGURE 3. QCM-D plot of frequency shift versus time for a silica coated-crystal bathed by the different RNIP suspensions at 0.20 wt% in 1 mM $NaHCO_3$. Note that all four polymer-modified RNIP suspensions show little change over the 70 min time period as compared with the unmodified RNIP sample. An expanded view of the polymer-modified RNIP data is available in the Supporting Information.

RNIP Adhesion to Silica. We investigated the effect of the polymer architecture on RNIP adhesion to silica for low and high ionic strength conditions. In each case, samples were chosen that corresponded to the plateau of the polymer adsorption isotherm to provide the most stringent possible comparison between polymers.

Figure 3 plots the third overtone frequency change during exposure of the silica surface to bare RNIP and each of four polymer-modified RNIP suspensions in 1 mM $NaHCO_3$ buffer. For the unmodified RNIP, there is a large decrease in frequency over the course of one hour. Multiple runs of this suspension yielded a range of adsorbed mass from 80 to 180 mg/m^2 indicating substantial adhesion of negatively charged RNIP to the negatively charged SiO_2 surface, in spite of the net electrostatic repulsion. This result agrees with previously published values for bare RNIP adhesion to SiO_2 using the QCM-D technique (*9*) and is consistent with the low mobility of bare RNIP in sand columns (*9, 13*).

Nominally treating RNIP as 50 nm diameter spheres (*1*) with a density of 7.86 g/cm^3 (for pure $Fe^{(0)}$) or 5.2 g/cm^3 (for pure magnetite, Fe_3O_4), the mass/area of a hexagonally close packed monolayer of pure $Fe^{(0)}$ or pure Fe_3O_4 particles that occupies 91% of the available surface area would be 131 mg/m^2 or 87 mg/m^2 respectively. This sets the upper and lower bound for the RNIP particles since these particles are composites of $Fe^{(0)}/Fe_3O_4$. While no claim is made as to the organization of the layer, this illustrates that RNIP adhesion is extensive and equivalent to a close packed monolayer.

All four of the different polyelectrolyte-modified RNIP samples show significant adhesion resistance to the silica surface, producing at most 0.25 mg/m^2 of adsorption, for PSS_{339}. This is negligible and would correspond to well below 1% of a monolayer. It is notable that the different polymer architectures used for these coatings showed essentially the same overall performance, despite the differing sizes of the PSS block and the different adsorbed amounts on RNIP.

In the presence of 50 mM NaCl, the greatest sensed mass for any of the polymer-modified RNIP samples was 0.47 mg/m^2 for the $PMAA_{15}$-$PBMA_{43}$-PSS_{811} sample, corresponding to just 0.5% of a monolayer. This small adsorbed amount was still within the apparent adsorbed amount that could be attributed to long-term drift in the instrument during these experiments. Unmodified RNIP suspensions rapidly flocculated in 50 mM NaCl and so could not be studied. Table 1 summarizes the QCM-D results along with the polymer adsorption data.

An increase in polyelectrolyte-modified RNIP adhesion to silica would be expected due to the additional charge screening provided by the 50 mM NaCl, had simple electrostatic double layer repulsion been responsible for the adhesion resistance. Whereas the Debye screening length (*30*) is 9.6 nm for the 1 mM ionic strength, it decreases to only 1.4 nm for 50 mM ionic strength. Since the elevated ionic strength had no significant effect on adhesion, it is more likely that electrosteric repulsion is the source of this lack of adhesion. This can explain the enhanced mobility of triblock copolymer-modified RNIP recently reported in saturated porous media at high salt concentration (*13*). Electrosteric repulsions, which can operate either between two opposing polyelectrolyte layers on interacting surfaces, or between one polyelectrolyte layer and an opposing bare, but charged, surface are known to remain strong even at elevated ionic strengths (*18*−*20*). The presence of the polyelectrolyte surface modifier on RNIP drastically reduces the amount of particle adhesion compared with the unmodified RNIP sample over a broad range of ionic strengths due to the robustness of electrosteric forces, rather than simple electrostatic forces.

These results are in good agreement with transport studies of bare RNIP in sand columns that show little elution of unmodified RNIP at comparable particle concentrations but extensive elution of polyelectrolyte-modified RNIP (*9, 13*). Unmodified RNIP elution is hindered by aggregation due to strong magnetic forces (*6*). Aggregates may grow in suspension to the point where they clog the porous medium (*9*). In addition, individual particles or small aggregates that adhere to the sand grains can continue to collect additional nanoparticles from suspension, and as those aggregates grow in size to fill pores, they can strain additional nanoparticles from the flowing suspension. Eliminating adhesion will weaken these tendencies.

Adhesion to Humic Acid Coated Surfaces. Natural organic matter (NOM), including humic acid, presents complex surface chemistries that could confound efforts to minimize RNIP adhesion in the subsurface. We used humic acid as a model for NOM to judge the effectiveness of the polyelectrolyte coatings under high organic content conditions. There has been previous research reported on the effects of humic acid on particle transport. When coated on mobile colloids, including hematite (*31*), kaolinite (*32*), and polymer latex (*33*), humic acid enhances colloidal transport through packed sand columns. In these three cases, humic acid was present in the bulk solution as well as adsorbed onto the colloidal particles. These studies show that humic acid is an effective surface modifier to enhance colloidal transport. Here we consider how humic acid coatings on the immobile surface influence particle adhesion.

Our first attempt to immobilize a humic acid layer was to merely adsorb it to the bare silica-coated QCM crystal, but it failed because all humic acid washed off during the rinse step. Given the negative charge on humic acid, a preadsorbed cationic polyelectrolyte layer on the silica surface could conceivably be used to bind humic acid. We chose not to use this strategy, since any exposed cationic sites could potentially cause adsorption of the anionic polyelectrolyte modified particles to the surface in a manner that would not be representative of humic acid interaction with polyelectrolyte modified RNIP. Instead we chose to first covalently bond a monolayer of electrically neutral, hydrophobic octadecyl chains to the silica crystal surface before exposing the surface to humic acids. This succeeded in creating an irreversibly bound humic acid coating, as shown in Figure 4. The stable humic acid surface concentration achieved here, ~1.5 mg/m^2, is typical of saturated polymer or surfactant layers (*15, 26*), but it is not known with certainty that no methyl termini of the underlying OTS monolayer are exposed. Nevertheless,

TABLE 1. Summary of Adsorption Isotherms and QCM-D Adhesion Results for Polymer Modified RNIP on SiO_2 for Two Ionic Strengths

sample	Polymer surface excess concentration (mg/m^2) for 1 mM $NaHCO_3$	Polymer surface excess concentration (mg/m^2) for 1 mM $NaHCO_3$ + 50 mM NaCl	Adhered mass (mg/m^2) on silica for 1 mM $NaHCO_3$	Adhered Mass (mg/m^2) on silica for 1 mM $NaHCO_3$ + 50 mM NaCl
unmodified RNIP	NA	NA	80−180	NA
$PMAA_{15}$-$PBMA_{43}$-PSS_{811}	1.6 ± 0.3	2.8 ± 0.6	−0.32 ± 0.23*	0.47 ± 0.30
$PMAA_{15}$-PSS_{811}	0.34 ± 0.1	0.7 ± 0.2	−0.35 ± 0.23*	−0.35 ± 0.27*
$PMMA_{45}$-PSS_{609}	1.3 ± 0.4	NA	0.21 ± 0.28	0.09 ± 0.11
PSS_{339}	0.26 ± 0.03	1.37 ± 0.3	0.25 ± 0.01	0.33 ± 0.18

(*) Samples with negative masses should not be thought of as "desorbed" amounts. The drift measured for a clean SiO_2 crystal was found to be ± 2.8 Hz or ± 0.5 mg/m^2 over the same time period as the experiments. Error bars are standard deviations of replicate experiments.

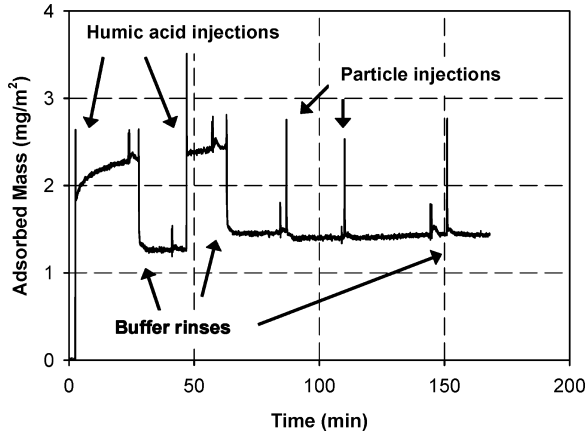

FIGURE 4. QCM-D plot of adsorbed mass versus time for humic acid adsorption onto OTS-coated SiO_2 followed by injection of 0.20 wt% $PMAA_{15}$-$PBMA_{43}$-PSS_{811} coated RNIP in 1 mM $NaHCO_3$. Arrows indicate time of injection for each material. The spikes in the plot are transient pressure-induced artifacts of injection and are not representative of any adsorption process.

this model presents the key features of NOM, a mix of anionic and neutral organic functionality.

Figure 4 shows a typical QCM-D experiment for the adsorption of humic acid onto OTS-coated surfaces in 1 mM $NaHCO_3$ buffer followed by injections of $PMAA_{15}$-$PBMA_{43}$-PSS_{811} coated RNIP in 1 mM $NaHCO_3$ buffer. Extraneous spikes in the plot occur when loading the temperature loop of the instrument with sample or from the actual injections into the sample chamber. They are not indicative of adsorption. For all experiments in 1 mM $NaHCO_3$ and 1 mM $NaHCO_3$ + 50 mM NaCl buffers, the final humic acid surface excess concentration was between 1−2 mg/m^2 and 1.8−2.7 mg/m^2 respectively.

After the final rinse, the triblock copolymer modified RNIP was injected into the sample chamber, resulting in a slight *decrease* in sensed adsorbed mass. The cause of this decrease is not known, but it may be a partial solubilization of humic acid by the polymer-coated particles in suspension. Upon repeated injections of the triblock copolymer modified particles, no measurable adhesion was observed. This indicates that the adsorbed polymer layer provides a sufficiently strong repulsion to prevent RNIP adhesion to humic acid coated surfaces. Every one of the polymer modified RNIP suspensions showed no detectable adhesion to the humic acid coated surface. In all experiments, we observed a slight loss of the bound humic acid upon injection of the suspensions but this had no adverse effect on particle adhesion. The absence of polymer-modified RNIP adhesion persisted in the presence of 50 mM NaCl, despite the increased electrostatic screening. Interestingly, we observed that unmodified RNIP also showed no adhesion to the humic acid film for the 1 mM $NaHCO_3$ case. The lack of bare RNIP adhesion to a humic acid coating may also be electrosteric in nature, given the macromolecular character of humic acid. This observation is consistent with the significantly slower deposition kinetics recently reported for bare fullerene nanoparticles on humic acid films (*34*). The possibility does exist that some humic acid desorbed from the film and subsequently transferred to RNIP in suspension and played some role in the adhesion resistance, but this remains to be tested. The lack of adhesion of bare RNIP to NOM coated silica suggests that bare RNIP may transport further in real aquifer materials where NOM is present compared to that predicted from laboratory column experiments in the absence of NOM (*9, 13*).

The different block copolymers and homopolymers had the same performance in resisting adhesion to the humic acid film for both low and high ionic strengths, and they had similar performances in resisting adhesion to a SiO_2 surface for the same ionic strength conditions, demonstrating their robustness. The common link between all of the polymers used is the strong polyelectrolyte block, PSS, that provides electrosteric repulsion from negatively charged surfaces. The observation that each polymer was equally effective in preventing adhesion does not mean that the strength of the electrosteric repulsion is independent of polymer composition and/or the adsorbed layer structure. Such forces are, in fact, quite sensitive to the layer structure (*18−20*). It simply means that in all cases, the resulting repulsion was *strong enough* to prevent adhesion even at elevated ionic strength.

These results indicate that PSS alone would be a sufficient surface modifier to prevent RNIP adhesion to silica or humic acid coated surfaces. While adhesion is not the sole determinant of NZVI mobility in groundwater, if any polymer that contained a PSS block were acceptable for minimizing adhesion and thereby promoting subsurface transport, then one might have considerable leeway in designing more sophisticated polymer architectures to impart other desirable functions. For example, hydrophobic blocks could be added to help anchor particles in a NAPL source zone. Finally, it should be noted that some soils have negatively charged minerals decorated to varying degrees by patches of positively charged iron oxides. These have been found to increase adhesion of negatively charged bacteria, but the effect is mitigated by adsorption of NOM (*35*) that reverts the surface back to a net negative charge (*31*). It remains to be determined how such patches, with or without NOM modification, would affect polyelectrolyte-modified NZVI adhesion.

Acknowledgments

This work is based on material supported by the National Science Foundation under grant BES-0608646 and EF-0830093, and by the U.S. EPA under grant number R833326.

Supporting Information Available

Adsorption isotherms, block copolymer synthesis, and NMR spectra of sulfonated polymers are provided. This material is available free of charge via the Internet at http://pubs.acs.org.

Literature Cited

(1) Li, X.-Q.; Zhang, W.-X. Sequestration of metal cations with zerovalent iron nanoparticles-A study with high resolution x-ray photoelectron spectroscopy (HR-XPS). *J. Phys. Chem. C.* **2007**, *111* (19), 6939–6946.

(2) Liu, Y.; Majetich, S. A.; Tilton, R. D.; Sholl, D. S.; Lowry, G. V. TCE dechlorination rates, pathways, and efficiency of nanoscale iron particles with different properties. *Environ. Sci. Technol.* **2005**, *39* (5), 1338–1345.

(3) Liu, Y.; Lowry, G. V. Effect of particle age (Fe0 content) and solution pH on NZVI reactivity: H_2 evolution and TCE dechlorination. *Environ. Sci. Technol.* **2006**, *40* (19), 6085–6090.

(4) Liu, Y.; Choi, H.; Dionysiou, D.; Lowry, G. V. Trichloroethene hydrodechlorination in water by highly disordered monometallic nanoiron. *Chem. Mater.* **2005**, *17* (21), 5315–5322.

(5) Liu, Y.; Phenrat, T.; Lowry, G. V. Effect of TCE concentration and dissolved groundwater solutes on NZVI-promoted TCE dechlorination and H_2 evolution. *Environ. Sci. Technol.* **2007**, *41* (22), 7881–7887.

(6) Phenrat, T.; Saleh, N.; Sirk, K.; Tilton, R. D.; Lowry, G. V. Aggregation and sedimentation of aqueous nanoscale zerovalent iron dispersions. *Environ. Sci. Technol.* **2007**, *41* (1), 284–290.

(7) He, F.; Zhao, D.; Liu, J.; Roberts, C. B. Stabilization of Fe-Pd nanoparticles with sodium carboxymethyl cellulose for enhanced transport and dechlorination of trichloroethylene in soil and groundwater. *Ind. Eng. Chem. Res.* **2007**, *46* (1), 29–34.

(8) Schrick, B.; Hydutsky, B. W.; Blough, J. L.; Mallouk, T. E. Delivery vehicles for zerovalent metal nanoparticles in soil and groundwater. *Chem. Mater.* **2004**, *16* (11), 2187–2193.

(9) Saleh, N.; Sirk, K.; Liu, Y.; Phenrat, T.; Dufour, B.; Matyjaszewski, K.; Tilton, R. D.; Lowry, G. V. Surface modifications enhance nanoiron transport and NAPL targeting in saturated porous media. *Environ. Eng. Sci.* **2007**, *24* (1), 45–57.

(10) Cantrell, K. J.; Kaplan, D. I. Zero-valent iron colloid emplacement in sand columns. *J. Environ. Eng. (New York)* **1997**, *123* (5), 499–505.

(11) Kanel, S. R.; Goswami, R. R.; Clement, T. P.; Barnett, M. O.; Zhao, D. Two dimensional transport characteristics of surface stabilized zero-valent iron nanoparticles in porous media. *Environ. Sci. Technol.* **2008**, *42* (3), 896–900.

(12) Quinn, J.; Geiger, C.; Clausen, C.; Brooks, K.; Coon, C.; O'Hara, S.; Krug, T.; Major, D.; Yoon, W.-S.; Gavaskar, A.; Holdsworth, T. Field demonstration of DNAPL dehalogenation using emulsified zero-valent iron. *Environ. Sci. Technol.* **2005**, *39* (5), 1309–1318.

(13) Saleh, N.; Kim, H.-J.; Matyjaszewski, K.; Tilton, R. D.; Lowry, G. V. Ionic strength and composition affect the mobility of surface-modified NZVI in water-saturated sand columns. *Environ. Sci. Technol.* **2008**, *42* (9), 3349–3355.

(14) Saleh, N.; Phenrat, T.; Sirk, K.; Dufour, B.; Ok, J.; Sarbu, T.; Matyjaszewski, K.; Tilton, R. D.; Lowry, G. V. Adsorbed triblock copolymers deliver reactive iron nanoparticles to the oil/water interface. *Nano Lett.* **2005**, *5* (12), 2489–2494.

(15) Phenrat, T.; Saleh, N.; Sirk, K.; Kim, H.-J.; Matyjaszewski, K.; Tilton, R. D.; Lowry, G. V. Stabilization of aqueous nanoscale zerovalent iron dispersions by anionic polyelectrolytes: adsorbed anionic polyelectrolyte layer properties and their effect on aggregation and sedimentation. *J. Nanopart. Res.* **2008**, *10* (5), 795–814.

(16) Cornell, R. M.; Schwertmann, U. *The Iron Oxides: Structure, Properties, Reactions, Occurrences and Uses*; VCH: Weinheim, Germany, 1996.

(17) Chibowski, S.; Wisniewska, M. Study of electrokinetic properties and structure of adsorbed layers of polyacrylic acid and polyacrylamide at Fe_2O_3-polymer solution interface. *Colloid Surf., A* **2002**, *208* (1−3), 131–145.

(18) Biesheuvel, P. M. Ionizable polyelectrolyte brushes: brush height and electrosteric interaction. *J. Colloid Interface Sci.* **2004**, *275* (1), 97–106.

(19) Pincus, P. Colloid stabilization with grafted polyelectrolytes. *Macromolecules* **1991**, *24* (10), 2912–2919.

(20) Balastre, M.; Li, F.; Schorr, P.; Yang, J.; Mays, J. W.; Tirrell, M. V. A study of polyelectrolyte brushes formed from adsorption of amphiphilic diblock copolymers using the surface force apparatus. *Macromolecules* **2002**, *35* (25), 9480–9486.

(21) Rodahl, M.; Hook, F.; Krozer, A.; Brzezinski, P.; Kasemo, B. Quartz crystal microbalance setup for frequency and Q-factor measurements in gaseous and liquid environments. *Rev. Sci. Instrum.* **1995**, *66* (7), 3924–30.

(22) Plunkett, M. A.; Claesson, P. M.; Ernstsson, M.; Rutland, M. W. Comparison of the adsorption of different charge density polyelectrolytes: a quartz crystal microbalance and x-ray photoelectron spectroscopy study. *Langmuir* **2003**, *19* (11), 4673–4681.

(23) Matyjaszewski, K.; Xia, J. Atom transfer radical polymerization. *Chem. Rev.* **2001**, *101* (9), 2921–2990.

(24) Wang, J.-S.; Matyjaszewski, K. Controlled/"living" radical polymerization. halogen atom transfer radical polymerization promoted by a Cu(I)/Cu(II) redox process. *Macromolecules* **1995**, *28* (23), 7901–7910.

(25) Sauerbrey, G. Z. Use of quartz crystal vibrator for weighting thin films on a microbalance. *Zeitschrift Fur Physik* **1959**, *155* (2), 206–222.

(26) Kumar, N.; Garoff, S.; Tilton, R. D. Experimental observations on the scaling of adsorption isotherms for nonionic surfactants at a hydrophobic solid-water interface. *Langmuir* **2004**, *20* (11), 4446–4451.

(27) van der Schee, H. A.; Lyklema, J. A lattice theory of polyelectrolyte adsorption. *J. Phys. Chem.* **1984**, *88* (26), 6661–6667.

(28) Velegol, S. B.; Tilton, R. D. A connection between interfacial self-assembly and the inhibition of hexadecyltrimethylammonium bromide adsorption on silica by poly-L-lysine. *Langmuir* **2001**, *17* (1), 219–227.

(29) Sontum, P. C.; Nævestad, A.; Fahlvik, A. K.; Gundersen, H. G. Adsorption of poly(sodium(4)styrenesulfonate) on colloidal iron oxide particles. *Int. J. Pharm.* **1996**, *128* (1,2), 269–275.

(30) Hiemenz, P. C.; Rajagopalan, R. *Principles of Colloid and Surface Chemistry*; Marcel Dekker: New York, 1997.

(31) Kretzschmar, R.; Sticher, H. Transport of humic-coated iron oxide colloids in a sandy soil: influence of Ca2+ and trace metals. *Environ. Sci. Technol.* **1997**, *31* (12), 3497–3504.

(32) Akbour, R. A.; Douch, J.; Hamdani, M.; Schmitz, P. Transport of kaolinite colloids through quartz sand: influence of humic acid, Ca2+, and trace metals. *J. Colloid Interface Sci.* **2002**, *253* (1), 1–8.

(33) Davis, C. J.; Eschenazi, E.; Papadopoulos, K. D. Combined effects of Ca^{2+} and humic acid on colloid transport through porous media. *Colloid Polym. Sci.* **2002**, *280* (1), 52–58.

(34) Chen, K. L.; Elimelech, M. Interaction of fullerene (C_{60}) nanoparticles with humic acid and alginate coated silica surfaces: measurements, mechanisms, and environmental implications. *Environ. Sci. Technol.* **2008**, *42* (20), 7607–7614.

(35) Johnson, W. P.; Logan, B. E. Enhanced transport of bacteria in porous media by sediment-phase and aqueous-phase natural organic matter. *Water Res.* **1996**, *30* (4), 923–931.

ES803589T